1162 | https://doi.org/10.3311/PPci.41037
Creative Commons Attribution

Periodica Polytechnica Civil Engineering, 69(4), pp. 1162–1175, 2025

The Effect of Different Block Shapes on the Downstream Local Scour in Piano Key Weir

Wadi Mohammed Wadi[1], Seyed Hamid Alavi[2], Elham Izadinia[3], Farnoosh Aghaee Daneshvar[4], Ali Khoshfetrat[5*]

[1] Department of Surveying, Southern Technical University, Zubair Road, 61001 Basra, Iraq
[2] Civil and Environmental Engineering Department, Tarbiat Modares University, 1463645851 Tehran, P.O.B. 14115-111, Iran
[3] Department of Civil Engineering, Faculty of Engineering and Technology, Shahid Ashrafi Esfahani University, 4999981798 Isfahan, Iran
[4] Department of Civil and Environmental Engineering, Shiraz University of Technology, 71557-13876 Shiraz, P.O.B. 71555-313, Iran
[5] Department of Civil Engineering, Isf.C., Islamic Azad University, 3999881551 Isfahan, P.O.B. 51595-158, Iran
* Corresponding author, e-mail: ali.khoshfetrat@iau.ac.ir

Received: 16 May 2025, Accepted: 18 September 2025, Published online: 01 October 2025

Abstract

Piano key weirs (PKWs) have a higher discharge capacity than their traditional form, the labyrinth weirs. Due to the high efficiency of PKW, the investigation of their downstream scour is important and requires mitigation strategies. For the first time, this study investigated scour reduction using different block shapes in the outlet keys of a C type trapezoid PKW. The shapes of the blocks are rectangular cubes, trapezoidal cubes (prisms), and cylinders. The range of the densimetric Froude number was between 1.038 and 2.903, while the range of the ratio of the total flow head upstream of the weir to its downstream was between 0.252 and 0.461. The findings revealed that scouring was reduced by 12.7 and 27.3% with an increase of 200 and 300% in the tailwater depth and by 14.5 and 29.3% with a 12.5 and 25% decline in the flow rate. Blocks in the outlet keys significantly reduced the maximum scour depth, with rectangular blocks being the most effective (55.7% reduction), followed by trapezoidal (32.2%) and circular (11.3%). Blocks also elongated the scour hole and shifted the maximum scour depth away from the weir toe. The scour index was lower in weirs with blocks, indicating reduced overturning risk.

Keywords

experimental investigation, outlet keys, PKW, scour index, type C

1 Introduction

Piano key weirs (PKWs) are a type of weir known for their high discharge efficiency. They come in four main types (A, B, C, and D) and can have rectangular, triangular, or trapezoidal plan geometries. Fig. 1 displays the types of PKW models. Type A weirs have one overhang in the upstream and downstream, type B and C weirs have one overhang in the upstream and downstream, respectively, while type D weirs have no overhang [1]. This design allows for a longer weir crest within a limited width, enabling significantly higher flow discharge compared to traditional weirs. The discharge coefficient in PKWs is 3–4 times greater than in conventional weirs [2]. Besides dams, these weirs find application in drainage channels and rivers. Loombah (Ryan's creek, Australia) and Gaddamvaripalli village (Andhra Pradesh, India) PKWs are situated in drainage channels and rivers, respectively [3, 4]. Due to the high efficiency of PKWs, it is crucial to conduct valuable studies on downstream scouring of these weirs. Many researchers have examined the hydraulic effect of flow on scouring in PKWs. Jüstrich et al. [5] found that for type A rectangular

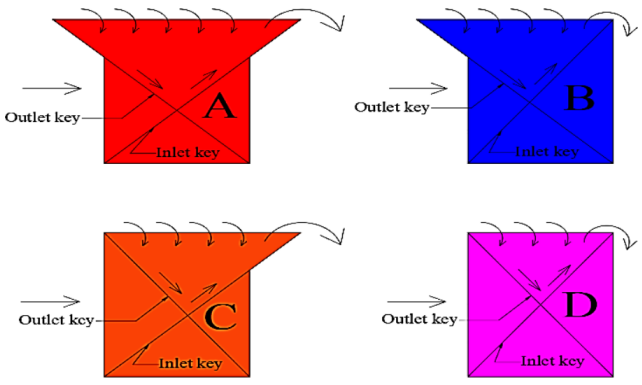

Fig. 1 All types (A, B, C and D) of PKWs from the side view

Cite this article as: Mohammed Wadi, W., Alavi, S. H., Izadinia, E., Aghaee Daneshvar, F., Khoshfetrat, A. "The Effect of Different Block Shapes on the Downstream Local Scour in Piano Key Weir", Periodica Polytechnica Civil Engineering, 69(4), pp. 1162–1175, 2025. https://doi.org/10.3311/PPci.41037

weirs, scouring grows with increase in the flow rate or flow fall height and drops with increase in tailwater depth or average diameter of bed particles. Ghafouri et al. [6] noted an increase in the maximum scour depth with increased flow rate and a reduction with increased tailwater depth for type A trapezoidal weirs. Bodaghi et al. [7] found that scouring in the submerged flow condition for type A trapezoidal weirs was significantly less than in free-flow conditions. The numerical simulation by Dehghan and Karami [8] indicated a reduction in the maximum scour depth for trapezoidal and triangular PKWs, by lowering discharge. Bodaghi et al. [1] found that in trapezoidal type A PKWs, elevation of the densimetric Froude number and reducing the flow submergence enhanced the scour depth. Many researchers have explored the effect of the geometry of PKWs on scour. Gohari and Ahmadi [9] observed an increase in the maximum scour depth with an increase in weir cycle numbers for type A rectangular weirs. Yazdi et al. [10] as well as Ghodsian et al. [11] compared scouring in type A rectangular, triangular, and trapezoidal weirs, finding that the maximum scour depth in trapezoidal weirs was less and farther from the weir toe than in rectangular and triangular weirs. Jamal et al. [12] found that reducing the weir height and increasing the ratio of inlet key width to outlet key width would lower the maximum scour depth for type C rectangular weirs. Dehrashid et al. [13] conducted laboratory and numerical investigations on the maximum scour depth in type D rectangular weirs. Yazdi et al. [14] compared scouring in type A rectangular and trapezoidal weirs, and found that the highest shear stress occurred near the point of impact of inclined jets in rectangular, as opposed to trapezoidal. Abdi Chooplou et al. [15] examined scour patterns downstream of PKWs with different geometries. They concluded that scour depth at trapezoidal weirs was notably shallower compared to rectangular and triangular weirs. Many researchers have explored the effect of various additional structures on the scouring of PKWs. Kumar and Ahmad [16] discovered that the presence of an apron reduces scouring in type A rectangular weirs. Lantz et al. [17] by introducing an apron downstream of type A rectangular weirs observed a reduction in maximum scour depth. They also proposed an optimal apron length of 1.5 times the weir height. Rdhaiwi et al. [18] observed that the presence of an apron would lower scouring in type C trapezoidal weirs. Abdi Chooplou et al. [19] in numerical and laboratory investigations for type A rectangular weirs with triangular-toothed crests found significantly lower maximum scour depth. Fathi et al. [20], by examining the local scour downstream of the type A stepped trapezoidal PKWs, found that the presence of steps in the weir outlet keys would diminish scour. Kazerooni et al. [21] found that flow splitters diminish scour downstream of the PKW and direct the maximum scour depth further away from the weir toe.

Considering the efficiency and high flow capacity of PKWs, it is important to investigate scouring and find solutions to lower it. Also, considering the conducted studies on downstream scouring of PKWs, research gaps of type C PKWs necessitate further study. Moreover, the influence of different block geometries on maximum scour depth has not been explored so far. Abdi Chooplou et al. [22] investigated baffles with cubic geometry in trapezoidal and rectangular type A PKWs outlet keys. They conducted their study with a fixed baffle (block) geometry. Moreover, the influence of different block geometries on maximum scour depth has not been explored so far. According to the above research, flow rate, tailwater depth, and bed material have a great influence on local scour. For this reason, this research utilized type C PKW with three flow rates, three tailwater depths, and two-bed materials. Furthermore, three blocks with different geometries – cylindrical, rectangular cuboid, and trapezoidal cuboid – were employed. However, to generalize the results to real conditions such as rivers and drainage canals, scouring of other types of PKWs under steady flow conditions was also investigated considering different arrangements of dominant parameter. Based on the present parametric study, using dimensional analysis and taking into account the dominant parameter of the bed materials, the different geometry of the blocks, and the hydraulic characteristics of the flow, relationships are obtained to estimate the maximum scour depth in steady flow conditions.

2 Dimensional analysis

Equation (1) presents the parameters affecting the downstream scouring of type C PKWs with blocks in their outlet keys. In Eq. (1), Z_s represents the maximum scour depth, X_s denotes the distance of maximum scour depth from the weir toe, q is the discharge per unit width upstream of the weir, H and Y reflect the sum of the upstream flow and the tailwater depth in the weir along with the kinetic energy head, respectively, ΔH symbolizes the difference in flow head upstream and downstream of the weir, ρ_w stands for water density, $\Delta\rho$ is a difference between the density of material (ρ_s) and the density of water, μ represents dynamic viscosity, σ stands for the surface tension coefficient, g signifies gravitational acceleration, d_{50} indicates the average particle diameter of the bed material, and S is the shape function of the blocks. Due to the fixed height of the blocks, their direct influence has been disregarded in Eq. (1). Further, Fig. 2 depicts the influential parameters on the downstream scouring of type C PKWs.

In Fig. 2, h and y_t are the flow depth upstream and downstream of the weir, V_1 and V_2 denote the flow velocity upstream and downstream of the weir, respectively, and P_d is the height of the bed material. The height of P_d is 1.5 times the height of the spillway, so that in the most severe tests (higher flow rate, lower tailwater depth, sandy bed materials, and unblocked weirs), scour does not reach the bottom of the flume.

$$Z_s, X_s = f\left(q, H, Y, \Delta H, \rho_w, \Delta\rho, \mu, \sigma, g, d_{50}, S\right) \tag{1}$$

Considering three repeating parameters, water density, discharge per unit width, and flow head difference upstream and downstream of the weir, the scour parameter are functions of Eq. (2) using the Buckingham π theory.

$$\left(\frac{Z_s}{\Delta H}, \frac{X_s}{\Delta H}\right) = f\left(\begin{array}{l} \dfrac{H}{\Delta H}, \dfrac{Y}{\Delta H}, \mathrm{Fr}, \mathrm{Re}, \mathrm{We}, \dfrac{\rho_s - \rho_w}{\rho_w} \\ = \dfrac{\Delta\rho}{\rho_w} = G - 1, \dfrac{d_{50}}{\Delta H}, S \end{array}\right) \tag{2}$$

Combining the parameters of the flow Froude number Fr = $q/(g\Delta H^3)^{0.5}$, with $(G-1)$, and $(d_{50}/\Delta H)$, results in the parameter (Frd = $q/[\Delta H^2 g(G-1)d_{50}]^{0.5}$), referred to as the densimetric Froude number. Additionally, by combining two parameters $(H/\Delta H)$ and $(Y/\Delta H)$, the parameter (Y/H) is obtained. Furthermore, due to the significant flow turbulence, Reynolds number (Re = $q\rho_w/\mu$ > 4000), and considering depths greater than 0.03 m, Weber number (We = $q^2\rho_w/\Delta H\sigma$) will be disregarded [23, 24]. In the dimensional analysis, due to the naturalness of the bed material the constant value of $(G-1)$ and the effect of this parameter on Frd, its direct presence in Eq. (3) was omitted. Nevertheless, the scour parameters become functions of the parameters in Eq. (3). The definition of hydraulic parameters and parameters related to bed materials in the present study are similar to the parameters found in most of the studies conducted on the scouring of PKWs (such as Jüstrich et al. [5], Fathi et al. [20], and Abdi Chooplou et al. [22]).

$$\left(\frac{Z_s}{\Delta H}, \frac{X_s}{\Delta H}\right) = f\left(\frac{Y}{H}, \frac{d_{50}}{\Delta H}, \mathrm{Frd}, S\right) \tag{3}$$

3 Cases and methods

Experiments were conducted in a flume 10 m long, 0.60 m wide, and 1.20 m high (Fig. 3 (a)). The flow, regulated by a monitor-equipped pump with a 0.01% error, passed through flow straighteners before entering the weir. The weir was installed 5.50 m from the channel's start. The flow was supplied by a submersible pump. Upstream of the weir, the flow was fully developed, considering a zero-channel slope. Velocity profiles were taken at distances of 3.5, 4 and 4.5 m from the beginning of the channel, with these profiles coinciding. Water temperature fluctuated between 8 and 13 °C. Flow depths upstream and downstream of the weir were measured by sensors on the channel, connected to a monitor displaying flow depth. Fig. 3 (b) and (c) displays the ultrasonic sensors

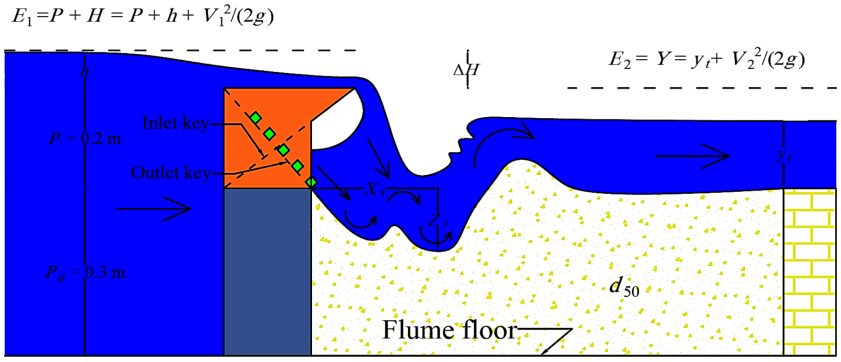

Fig. 2 Influential parameters on downstream scour of PKW type C with different block shapes

(a) (b) (c)

Fig. 3 Characteristics of laboratory channel and ultrasonic sensors: (a) Laboratory flume, (b) Ultrasonic sensors, (c) Programmable Logic Controller (PLC) device

and display device (PLC). Measurements were taken at 4h distance upstream of the weir's crest and 10P distance downstream [25], using a point gauge with a precision of 0.001 m. The measured depths from sensors and point gauge exhibited minimal error.

A type-C PKW with a height of 0.20 m was utilized, featuring inlet key width (W_i) of 0.215 m, outlet key width (W_o) of 0.075 m, sidewall length (B) of 0.495 m, weir crest length (L) of 2.56 m, and thickness (T_s) of 0.01 m (Fig. 4). The tailwater depth was artificially adjusted using an end gate. Three depths of 0.05, 0.10, and 0.15 m were used for the tailwater depths to ensure the flow over the weir remained non-submerged [26]. Discharges of 0.030, 0.035, and 0.040 m^3/s were employed. At the lowest discharge (0.030 m^3/s), the upstream weir depth exceeded 0.03 m. According to Fig. 5, three different block geometries rectangular, circular, and trapezoidal were used. Each outlet key contained nine complete blocks measuring 0.025 by 0.025 by 0.06 m and two half-sized blocks with the same height at the sides. All blocks were installed in the outlet keys as shown in Figs. 6 (a) and (b). The first block was placed to have minimal impact on discharge coefficient, upstream depth, or backflow. The block design concept was akin to baffled weirs [27]. Blocks were installed in a grid pattern on the outlet keys. Similar to

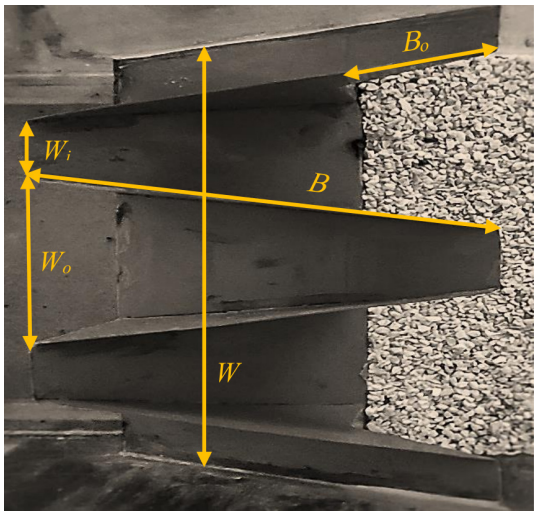

Fig. 4 PKW type C

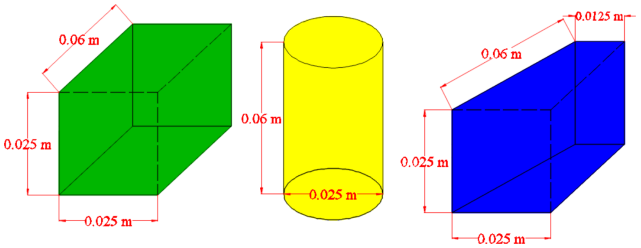

Fig. 5 Geometry of the blocks used in the study

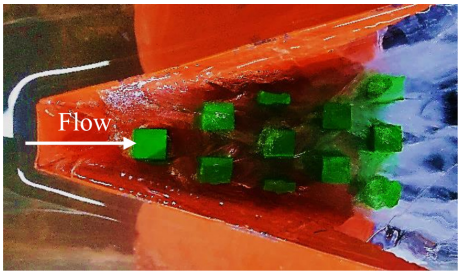

(a)

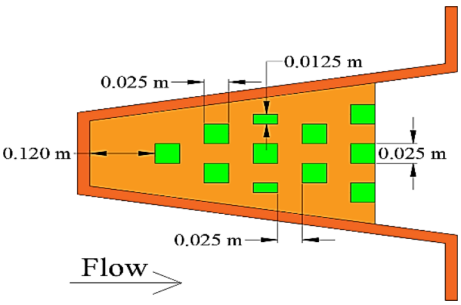

(b)

Fig. 6 Installed shape of the blocks in the weir outlet keys: (a) Experimental design; (b) Schematic design

baffled weirs, block placement on the outlet keys followed a zigzag pattern. All blocks had a similar configuration. Table 1 reports the hydraulic characteristics and sedimentation details of tests in weirs without blocks and Table 2 reveals the range of hydraulic characteristics and sedimentation details of tests in weirs with blocks, showing Q as the flow rate. In Tables 1 and 2, N refers to the weir without blocks, R denotes the weir with rectangular blocks, T stands for the weir with trapezoidal blocks, and C shows the weir with circular blocks. All hydraulic specifications across experiments were identical. Having upstream weir flow depths and flow rates, the flow velocity was estimated. Further, utilizing the continuity equation and the tailwater depth, tailwater velocity was computed. Gravel with an average particle size of 0.0075 m and sand with an average size of 0.0035 m were employed in the bed. The values of d_{50}/P used in the study by Jüstrich et al. [5] ranged from 0.01 to 0.04. In the present study, the value of d_{50}/P for gravel materials was 0.0375, and for sand materials, it was 0.0175. Therefore, the present study adopts a comparable range to facilitate a direct comparison with these foundational results. Scour depth for blocked weirs was only examined on the gravel bed. Eighteen tests were conducted on weirs without blocks using sand and gravel materials. Additionally, 27 tests were performed on blocked weirs using gravel materials. As per Tables 1 and 2, a total of 45 tests were conducted to measure the scour depth. A 16 h test was conducted for gravel and

Table 1 Hydraulic characteristics of flow in weir without blocks

Number of tests	Q (m^3/s)	H (m)	Y (m)	Bed materials	Block shape (S)	H/Y (–)	Y/H (–)	$d_{50}/\Delta H$ (sand)	$d_{50}/\Delta H$ (gravel)	Frd (sand)	Frd (gravel)
2	0.030	0.039	0.101	Gravel – sand	*N*	0.389	2.571	0.025	0.054	1.519	1.038
2	0.035	0.048	0.119	Gravel – sand	*N*	0.401	2.493	0.027	0.058	1.907	1.303
2	0.040	0.057	0.141	Gravel – sand	*N*	0.402	2.487	0.030	0.065	2.416	1.650
2	0.030	0.039	0.113	Gravel – sand	*N*	0.348	2.871	0.028	0.059	1.660	1.134
2	0.035	0.048	0.117	Gravel – sand	*N*	0.408	2.450	0.027	0.057	1.877	1.282
2	0.040	0.057	0.123	Gravel – sand	*N*	0.461	2.169	0.026	0.056	2.092	1.429
2	0.030	0.039	0.156	Gravel – sand	*N*	0.252	3.964	0.042	0.090	2.513	1.716
2	0.035	0.048	0.158	Gravel – sand	*N*	0.304	3.293	0.039	0.083	2.718	1.856
2	0.040	0.057	0.160	Gravel – sand	*N*	0.353	2.831	0.036	0.077	2.903	1.983

Table 2 The range of hydraulic flow changes in weirs with blocks

Desired parameter	Minimum	Maximum
Q (m^3/s)	0.030	0.040
H (m)	0.039	0.057
Y (m)	0.101	0.160
H/Y	0.252	0.461
Y/H	2.169	3.964
$d_{50}/\Delta H$	0.054	0.090
Fr	0.340	0.354
Frd (gravel)	1.038	1.983
Block shape (S): *R*, *T*, *C*		

sand materials separately. For gravel materials after 2.5 h and for sand materials after 4.5 h, the bed changes were less than 1 mm. For this reason, these times were considered as equilibrium times [28]. The uniformity coefficient ($\sigma_g = (d_{84}/d_{16})^{0.5}$) for bed materials used in the experiments was less than 1.6, indicating a uniform distribution of sand and gravel in the bed [29, 30]. The uniformity coefficient is 1.26 for sand materials and 1.19 for gravel materials. Before the experiments, a lightweight metal sheet was placed on the bed to prevent initial scouring. Once the tailwater depth and flow rate were set, this sheet was gradually removed. After reaching equilibrium, the pump was turned off, and a laser meter was utilized to survey the width and length of the channel. The bed was flattened before each test.

4 Results and discussion

4.1 Laboratory observations

The flow transitions freely as jets from the inlet keys downstream and leans as inclined jets from the outlet keys downwards. Upon flow transition from the inlet to the outlet keys, vortexes are induced along the sides, creating helical eddies. These side vortexes rotate clockwise and counterclockwise. According to Fig. 7, the side vortices on the right side of the outlet keys continue their path counterclockwise, and the side vortices on the left side of the outlet keys continue their path clockwise and enter the downstream bed superficially. The velocity of vortexes diminishes after their collision into the blocks in the outlet key. A small submerged region forms at the beginning of the outlet keys due to the convergence of the flow from the inlet keys toward the outlet. Additionally, a middle vortex exists within the outlet keys. The primary factor contributing to the middle vortex might be a submerged zone. As the flow velocity grows, this area becomes larger. The initial block beneath the submerged region propels the flow toward the center of the outlet keys. The velocity of the middle jet significantly surpasses that of the side vortexes [20]. Fig. 7 also shows the local submerged area in the outlet keys. To better represent the local submerged zone, a dye was gently introduced into the flow from the upstream of the weir. After the first block collision, the flow slightly reverses and splits. Following the split, the flow is directed downwards from both sides of the block, encountering the second-row blocks on its way. The flow separation continues until the end of the blocks, lowering the flow velocity. Fig. 8 displays the flow separation by tapping the middle blocks. The collision, separation, and merging of the flow with the separated flow from the side block generate weak vortexes. These vortexes occur at the lower surface of the flow and relatively close to the bed of the outlet keys.

Fig. 7 Local submerged area and side eddies present in the outlet keys of the weir

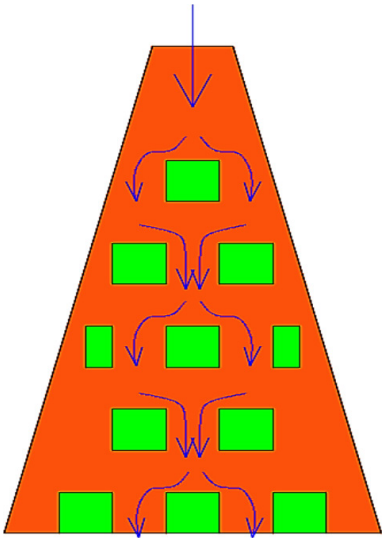

Fig. 8 Flow between intermediate blocks in the outlet key

The weak vortexes contribute to increased energy loss, ultimately leading to reduced velocity [25].

4.2 Energy loss

Researchers such as Sajadi [31], Al-Shukur and Al-Khafaji [32], Naghibzadeh et al. [33], Eslinger and Crookston [34], Singh and Kumar [35], Shen and Oertel [36], and Rdhaiwi et al. [37] have provided valuable insights into strategies for increasing energy loss. Fig. 9 illustrates the average energy loss ratio ($E_L = (E_1 - E_2)/E_1$) in weirs with and without blocks. As mentioned, the flow depth upstream of the weir and tailwater was measured using sensors and point gauges. Given the flow rate and the corresponding depth at the weir's upstream, the flow velocity at the upstream and the specific energy of the flow at the upstream $\left(E_1 = H + P = P + h + \left(V_1^2/2g\right)\right)$ can be calculated. Further, utilizing the continuity equation and the depth of tailwater, the downstream flow velocity and the specific energy of the flow at the tailwater $\left(E_2 = Y = y_t + \left(V_2^2/2g\right)\right)$ can be determined. As apparent in Fig. 9, the energy loss in weirs with rectangular cube blocks is significantly higher compared to other weirs. This might be attributed to the collision of the flow with the back of the block and its split into two directions, resulting in a decline in the flow velocity. In weirs with circular blocks, the energy loss is lower, likely due to the flow smoothly impacting the back of these blocks. In weirs with trapezoidal blocks, due to their inclined shape, the flow rises behind the blocks and is thrown downstream, without any flow colliding with the back of these blocks. Nevertheless, the energy loss in weirs with rectangular, circular, and trapezoidal blocks compared to the weirs without blocks rises by approximately 17.3%, 11.6%, and 14.6%, respectively.

Fathi et al. [25] conducted a valuable study on energy loss in stepped PKWs. The weir examined in their work was a type A trapezoidal PKW with a height of 0.2 m. Their study revealed that the average energy loss in 5-, 10-, and 15-stepped weirs compared to the weir without steps was approximately 15.73%, 24.93%, and 18.52%. The energy loss in their 0-step weir was about 5.4% higher compared to the current research's weir without block. Under the optimal condition of the current research, namely, with rectangular block geometries in the 10-step weir, the energy loss was approximately 14.4% lower compared to their best condition, the 10-stepped weir. Also, it can be concluded that the energy loss in type A and C weirs with constant heights is relatively similar, but in stepped weirs, the energy loss is significantly higher. Nevertheless, the comparison and investigation of flow energy loss needs further investigation and consideration of the boundary conditions of weirs.

4.3 Maximum scour depth, longitudinal profile of bed, and parameters affecting them

Fig. 10 (a) depicts the flatbed of materials. The length of the material used downstream of the weir (X) is 2.50 m. The surface of the bed material is precisely leveled, and then the tests are started. Also, with the steeper slope in the outlets compared to the inlets of the weir, a scour

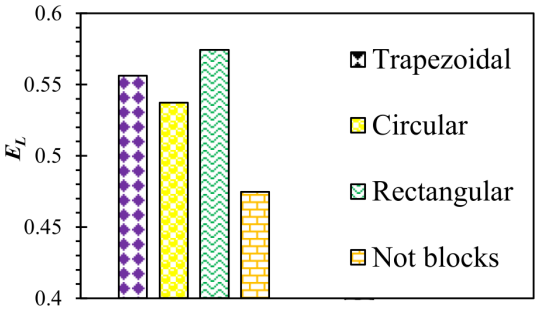

Fig. 9 Comparison of average energy loss in weir with and without blocks

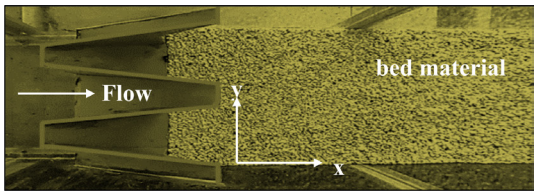

(a)

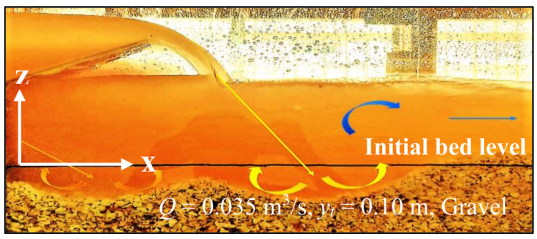

(b)

Fig. 10 PKW downstream bed materials: (a) Flat bed materials downstream of the weir before the start of the test; (b) Slope of the scour hole downstream of the PKW type C spillway after the start of the test

hole forms near the weir's crest. Due to the overhanging edge at the downstream end of the weir, the flow tends to jet towards the bed from the inlet side, causing turbulence in this area. This turbulence causes the material to be pushed back toward the weir toe, making the downstream scour slope even steeper. In the area where the flow cascades from the overhanging edge of the inlet to the bed, gravel particles are slightly more bulged (Fig. 10 (b)). The material being pushed back contributes to filling the scour hole created by the flow exiting from the weir's outlets. Hence, the maximum scour depth will be farther away from the weir crest. Additionally, with the presence of blocks and the reduction in flow velocity in the outlet keys, the initial scour hole or the one near the weir crest is shorter and shallower compared to the condition without blocks, while the maximum scour depth is observed in a farther hole. Also, according to the explanation given above, the scour hole becomes similar to the cosine curve.

Fig. 11 demonstrates the impact of Frd, *Y*/*H*, as well as different bed materials on the maximum scour depth. Fig. 11 (a) displays the effect of Frd on the maximum scour depth. Fig. 11 (a) presented for a weir without blocks, using gravel as the bed material, and a constant tailwater depth of 0.05 m. As observed, an increase in Frd leads to a rise in the maximum scour depth. As Frd increases, so does the flow rate. Also, with the increase in the flow rate, the flow shear stress exceeds the critical shear stress and causes an increase in the maximum scour depth. The reason behind this could be the increased flow velocity and the amplified outward jets from the inlet and outlet keys towards the downstream bed. For a weir without block with gravel as the bed material, on average, with an increase of 16.7% and 33.3% in flow rate compared to a flow rate of 0.03 m^3/s, the maximum scour depth grows approximately by 21.5% and 35.2%. Fig. 11 (b) exhibits the effect of tailwater depth on the maximum scour depth. Fig. 11 (b) presented for a weir without blocks, using gravel as the bed

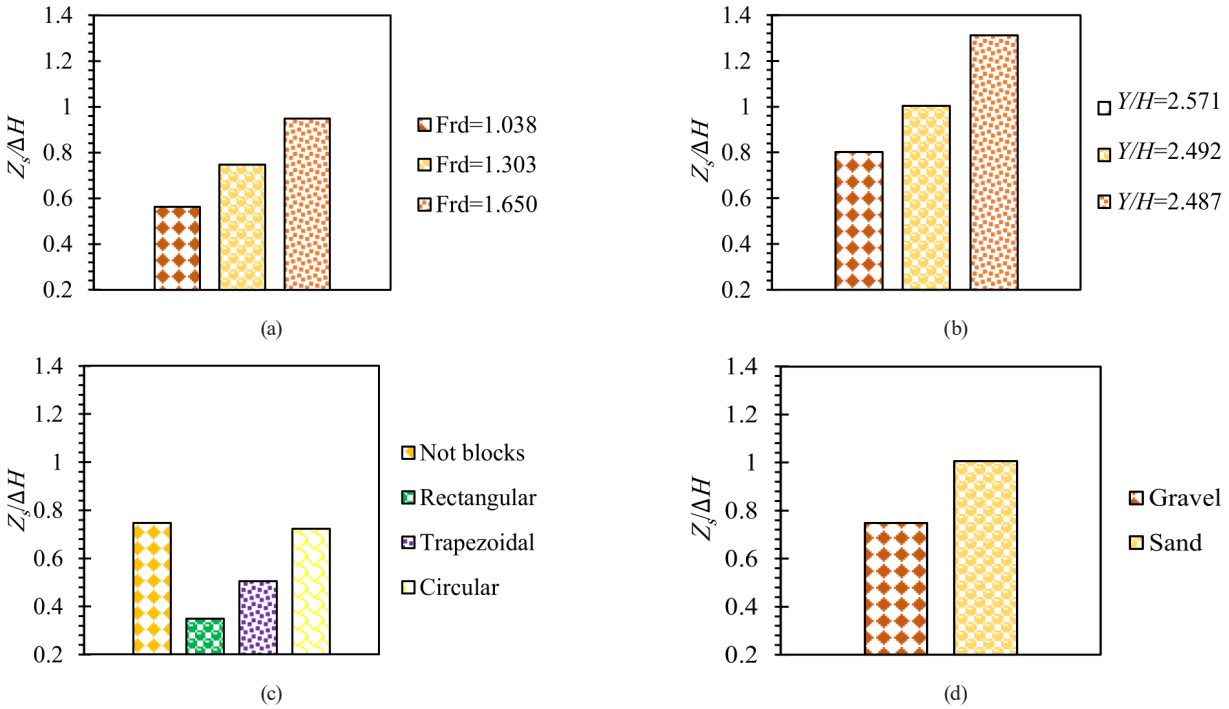

Fig. 11 Effect of parameter such as: (a) Frd; (b) *Y*/*H*; (c) Block shape; (d) Material diameter on maximum scour depth

material, and a constant flow rate of 0.04 m^3/s. As observed, an increase in the tailwater depth results in a reduction in the maximum scour depth. The cause could be the reduced flow velocity downstream and its impact on the velocities created from the combination of outlet jets from outlet keys and vortexes in the scour hole. As the tailwater depth increases, the flow downstream of the weir has a lower velocity, and with its mixing with the outlet flow from the weir, it calms down the flow and lowers its velocity, and the shear stress is close to the critical shear stress and mitigates scour. As the depth of the tailwater increases, so does the propagation length of the jets hitting the bed material [38–40]. As the propagation length increases and the existing jets as well as eddies become shallower, the maximum scour depth drops, and the scour becomes shallower and more stretched. Also, the power of the hydraulic jump also diminishes, and the hydraulic jump becomes shallower and can be considered submerged [41–43]. For a weir without block with gravel, as the bed material, on average, with a 2 and 3-times increase in tailwater depth compared to a depth of 0.05 m, the maximum scour depth falls by 11.3% and 23.9%. Fig. 11 (c) depicts the impact of different blocks geometries on the maximum scour depth. Fig. 11 (c) outlined for a constant flow rate and tailwater depth, using gravel as the bed material. As can be seen, the maximum scour depth diminishes with the presence of blocks. Furthermore, the maximum scour depth in weirs with rectangular blocks is notably lower than in other weirs. The cause could be higher energy loss in these weirs, resulting in reduced outflow velocities from their outlet jets. Following weirs with rectangular blocks, the maximum scour depth in weirs with trapezoidal and circular blocks is lower compared to weirs without blocks. On average, the maximum scour depth in weirs with rectangular, trapezoidal, and circular blocks is approximately 55.7%, 32.2%, and 11.3% less than in weirs without blocks. Fig. 11 (d) demonstrates the impact of bed material gradation on the maximum scour depth. Fig. 11 (d) presented for constant flow rate and tailwater depth in weir without blocks. As depicted, reduction of the diameter of the bed material leads to an increase in the maximum scour depth [20]. The reason could be the smaller size of sand grains compared to gravel particles. Smaller particles can be easily transported downstream. The flow can easily transport and move smaller particles downstream. From a practical point of view, excessive shear stresses can lead to significant scour depths [44]. Over time, an armor layer forms on the gravel bed that prevents further scouring and reduces the shear stress on the gravel bed. With the increase in the diameter of the bed grains, the flow shear stress has less effect on scouring and cannot easily move larger grains. Also, the scouring phenomenon continues until the shear stress applied to the bed becomes critical. On average, in a weir without a block, the maximum scour depth in gravel bed materials, with a 53.3% increase in material diameter, is approximately 28.1% less than in sand bed materials.

Fig. 12 indicates the effects of various parameters on the maximum scour depth and longitudinal profile of the channel bed. Fig. 12 (a) illustrates the impact of Frd on the longitudinal scour profile for a weir without block with a constant tailwater depth of 0.05 m and gravel materials. As the Frd increases, so does the length of the scour hole due to the higher velocity of outlet jets over the weir and increased sediment transport downstream. Further, with the increase in the flow rate, the maximum scour depth at the weir toe grows, while the gravel mound height falls [20].

Fig. 12 (b) depicts the influence of tailwater depth on the longitudinal scour profile for weir without blocks with a constant discharge of 0.04 m^3/s and gravel materials. Augmentation of the tailwater depth, probably by preventing the length of diffusion and transport of sediment downstream and reducing the critical velocity in the sediment bed, will significantly reduce the length of the scour hole. Additionally, an increase in tailwater depth lowers the maximum scour depth at the weir toe, with minimal differences in gravel mound height. As the depth of the tailwater increases, so does the propagation length of the jets hitting the bed material. As the propagation length increases and the existing jets and eddies become shallower, the maximum scour depth decreases, and the scour becomes shallower and more stretched, and the power of the hydraulic jump also diminishes, and the hydraulic jump becomes shallower and can be considered submerged [20, 30].

Fig. 12 (c) reveals the effect of block shapes on the longitudinal scour profile with a constant discharge of 0.035 m^3/s, a tailwater depth of 0.05 m, and gravel materials. Despite the presence of blocks at the weir outlet keys, the scour hole becomes more inclined and extensive. Scour holes in rectangular, trapezoidal, and circular block weirs are considerably elongated and larger than those without blocks. Block shapes have an insignificant impact on the height of the scour mounds but reduce the maximum scour depth at the weir toe. The lowest scour depth was observed in rectangular block weirs.

Fig. 12 (d) illustrates the impact of material diameter on the longitudinal scour profile for a weir without blocks,

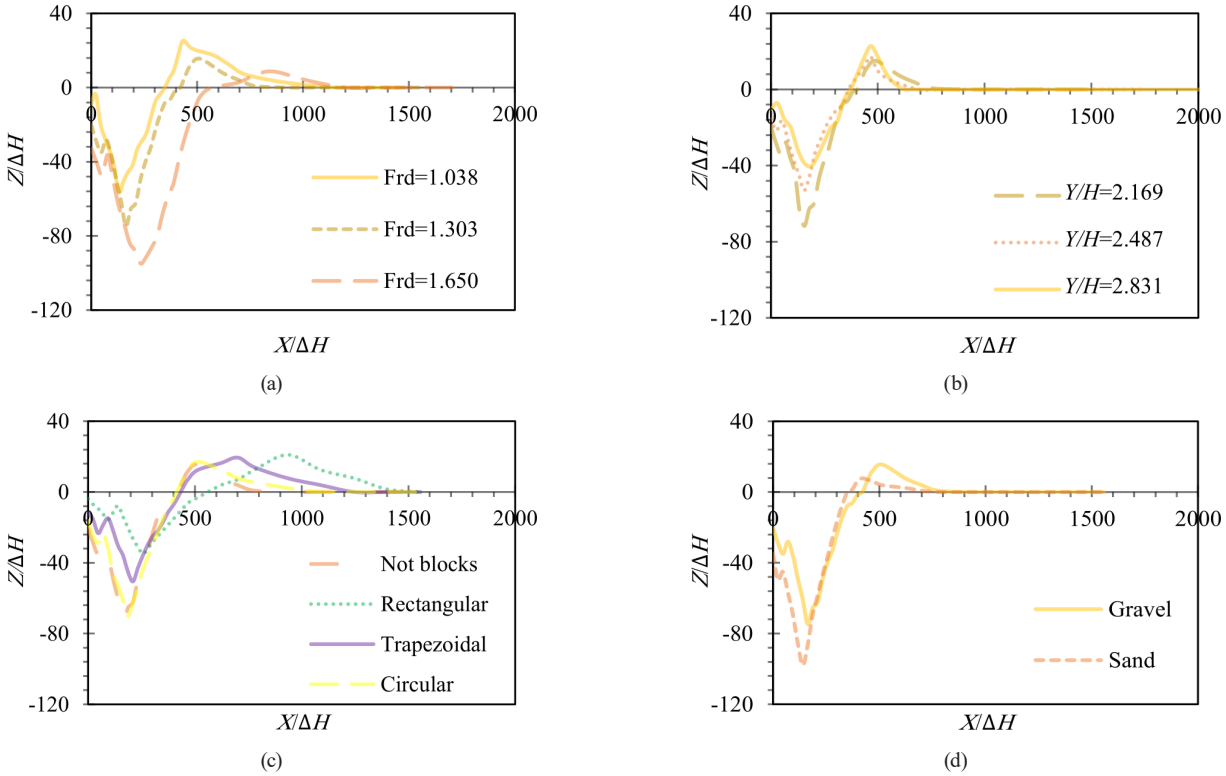

Fig. 12 Effect of: (a) Frd; (b) *Y/H*; (c) Block shape; (d) Material diameter on longitudinal scour profile

a constant tailwater depth of 0.05 m, and a constant discharge of 0.035 m^3/s. Reduction of the average particle diameter of the bed material enlarges the length of the scour hole, likely due to the lighter and finer nature of sand materials, promoting increased downstream sediment transport. Further, the location of the maximum scour depth in sand materials is closer to the weir toe. The maximum scour depth in sand materials exceeds that in the weir toe and gravel materials. Additionally, the mound heights in gravel materials are significantly lower than in sand materials.

Fathi et al. [20] combined the hydraulic parameters of the flow and the diameter of the bed material ($Y/\Delta H$, $H/\Delta H$, and $d_{50}/\Delta H$) and the equation obtained to calculate the maximum scour depth. In the present study, the hydraulic parameters of the flow and the diameter of the bed material were combined. Equation (4) is presented to calculate the maximum scour depth, exhibiting a correlation coefficient of 98.1%. In Eq. (4), the parameter K_1 represents the geometry function related to the shapes of the blocks, as discussed in Table 3. Furthermore, Fig. 13 illustrates the dimensionless observed and calculated values of the maximum scour depth. As evident, Eq. (4) with an error margin of (±20%) is acceptable for calculating the maximum scour depth in weirs both with and without blocks. Based on Fig. 13, Eq. (4) has also been used for the data of Rdhaiwi et al. [18]. They used the PKW type C in gravel materials with an average particle diameter similar to the current study, with an average maximum scour depth of 0.125 m with a USBR type I stilling basin and 0.062 m without it. As mentioned, the average maximum scour depth in the current study for weirs without blocks in gravel and sand materials is 0.084 m and 0.116 m. The difference in the maximum scour depth value between the study by Rdhaiwi et al. [18] and the current study is due to different hydraulic and laboratory conditions. Also, under the optimal condition (i.e., weir with rectangular blocks), the maximum scour depth is about 28.9% higher than the weir with USBR type I stilling basin (apron). Despite

Table 3 Calculation of coefficient K_1

Row	Block shape (*S*)	$d_{50}/\Delta H$	K_1	Root mean square error (RMSE)	Mean square error (MSE)	R^2 (%)
1	*N*	$0.025 < d_{50}/\Delta H < 0.090$	0.54	0.105	0.009	98.8
2	*R*	$0.054 < d_{50}/\Delta H < 0.090$	0.25	0.109	0.015	97.4
3	*T*	$0.054 < d_{50}/\Delta H < 0.090$	0.39	0.101	0.012	99.2
4	*C*	$0.054 < d_{50}/\Delta H < 0.090$	0.47	0.112	0.017	97.0

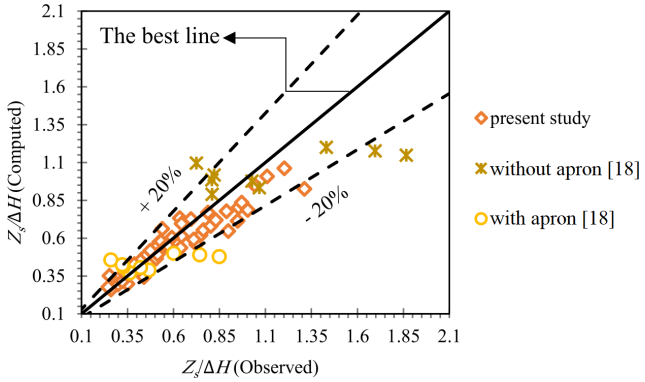

Fig. 13 Observed and calculated maximum scour depths

the slight difference in the maximum scour depth value, the presence of blocks is recommended. USBR type I stilling basin should be accompanied by a cutoff-wall and consisting of a large volume of concrete, which may not be environmentally friendly and economical.

$$\frac{Z_s}{\Delta H} = K_1 \left(\mathrm{Frd}^{0.49} \left(\frac{HY}{d_{50}\Delta H} \right)^{0.02\ \mathrm{Frd}} \right) \tag{4}$$

4.4 The maximum distance of scouring depth to the weir toe

Equation (5) with a correlation coefficient of 99.5% is provided to calculate the maximum distance of scour depth from the weir toe based on the calculated maximum scour depth using Eq. (4). The coefficient K_2 in Eq. (5) represents the function of block shape and material diameter, to be derived from Table 4. The maximum distance of scour depth in a bed of sand material is significantly closer to the weir toe compared to the maximum distance of scour depth in a bed of gravel material. Further, with the presence of blocks in the outlet keys and the reduction in flow velocity, the scour hole becomes elongated. Additionally, in weirs with blocks, the maximum distance of scour depth is farther from the weir toe. On average, with a 53.3% increase in material diameter, the maximum distance of scour depth compared to the weir toe is approximately 18.5% greater than the maximum distance of scour depth in sand bed material. As mentioned, the maximum distance of scour depth increases concerning the weir toe in the presence of blocks. Furthermore, the maximum distance of scour depth concerning the weir toe in rectangular block weirs is notably farther than in other weir types. Similar to the maximum scour depth in this weir, the increased value of the maximum distance of scour depth concerning the weir toe could be due to a higher energy loss in this weir, resulting in a reduced discharge velocity from its outlet jets. After the rectangular block weir, the maximum distance of scour depth concerning the weir toe is greater in trapezoidal and circular block weirs compared to weirs without blocks. On average, the maximum distance of scour depth concerning the weir toe in rectangular, trapezoidal, and circular block weirs is approximately 21.1%, 15%, and 8.3% greater than in weirs without blocks. Additionally, with an increase in tailwater depth, the maximum distance of scour depth concerning the weir toe will decline, while an increase in flow rate will move this distance farther from the weir toe. Fig. 14 illustrates the calculated and observed values of the maximum distance of scour depth concerning the weir toe, which is acceptable within an error margin of (±8%) and warrants further investigation.

$$\frac{X_s}{\Delta H} = K_2 \left(\frac{Z_s}{\Delta H} \right) \tag{5}$$

4.5 Scouring index

The scour index is a significant parameter in scour analysis, defined as the ratio of twice the maximum scour depth to the distance of maximum scour depth relative to the weir toe ($S_i = 2Z_s/X_s$). A lower scour index implies a reduced risk of weir failure [45, 46]. A lower scour index can result from either a smaller maximum scour depth or a greater distance from the weir toe. Referring to Fig. 15, the average scour index in weirs without blocks using sand material is approximately 41.9% larger than in weirs without blocks using gravel material. Additionally, the average scour index in rectangular, trapezoidal, and circular block

Table 4 Calculation of coefficient K_2

Row	Block shape (S)	Bed materials	$d_{50}/\Delta H$	K_2	RMSE	MSE	R^2 (%)
1	N	Sand	$0.025 < d_{50}/\Delta H < 0.042$	1.513	0.118	0.015	99.6
2	N	Gravel	$0.054 < d_{50}/\Delta H < 0.090$	2.141	0.106	0.008	99.7
3	R	Gravel	$0.054 < d_{50}/\Delta H < 0.090$	6.849	0.112	0.012	99.3
4	T	Gravel	$0.054 < d_{50}/\Delta H < 0.090$	4.065	0.114	0.014	99.2
5	C	Gravel	$0.054 < d_{50}/\Delta H < 0.090$	3.096	0.109	0.011	99.6

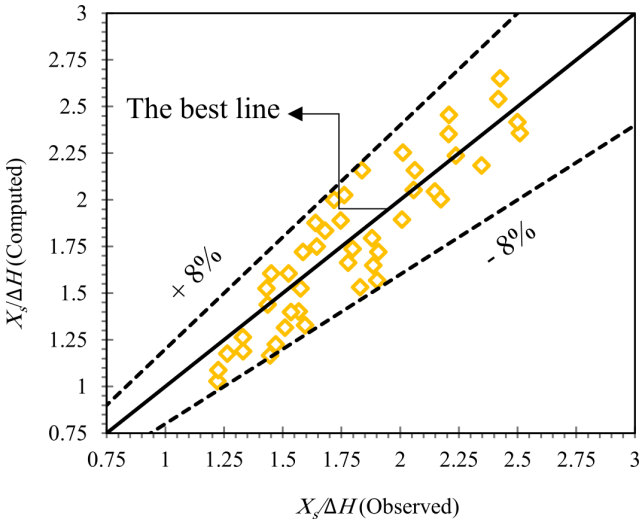

Fig. 14 Observed and calculated distances of maximum scour depth relative to weir toe

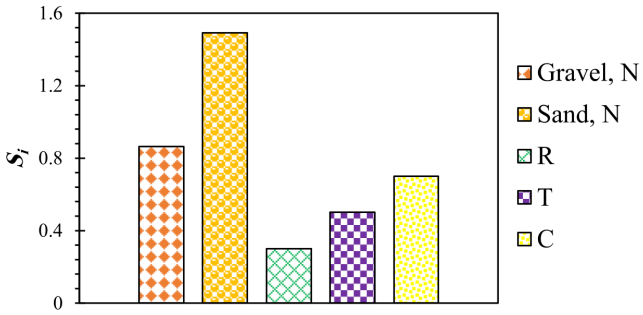

Fig. 15 Scour index in weir with and without blocks

weirs using gravel material is approximately 65.1%, 42.1%, and 19.1% smaller, compared to weirs without blocks using gravel material. However, the most optimal scenario for the scour index was observed in rectangular block weirs. Jüstrich et al. [5] investigated the scour of rectangular PKWs type A and found that as the flow rate and flow drop height increased and the tailwater depth and the material diameter decreased, the maximum scour depth rose. Their weir height was 0.15 m. They conducted six tests using sand materials with a flow drop height equal to the weir height. Their average scour index was 1.492.

In the present study, the average scour index for sand materials has been 1.490, with an error of 0.13%, equivalent to the average scour index in the Jüstrich et al. [5] study. The average scour index in the research of Lantz et al. [47] by examining the rectangular PKW type A with an average bed diameter of 0.0065 m was equal to 1.71. The average scouring index in the PKW in the present study has been about 49.4% lower than the average scouring index in the research of Lantz et al. [47]. Also, the average scouring index in the research of Ghodsian et al. [11] was approximately equal to 2 and in the research of Yazdi et al. [10], it was around 1.65. In the present research, the value of scouring index and gravel materials is about 56.7 and 47.5%, and in sand materials about 25.5 and 9.7% less than the research of Ghodsian et al. [11] and Yazdi et al. [10]. The reason for the reduction of the scour index in the current research could be the flow falling at a distance far from the weir toe or the larger diameter of the bed material.

5 Conclusions

Scour reduction is crucial for preventing hydraulic structure collapse. Similar to applications in baffled weirs and stilling basins, this study demonstrated that blocks in the outlet keys of C type PKWs significantly reduced scour depth and increased energy loss. Rectangular blocks were the most effective, followed by trapezoidal and circular. The rectangular blocks would act as a barrier in front of the flow. Still, due to the slope of the trapezoidal blocks as well as the circular blocks acting like a cylinder, the flow would pass easily, and there would be less reduction of the flow velocity. Blocks also elongated the scour hole and shifted the maximum scour depth away from the weir. This approach offers potential for application in natural environments and various weir designs (Ogee, Chute, Crump, and other PKW types). Also, the range of the densimetric Froude number was between 1.038 and 2.903, and the range of the ratio of the total flow head upstream of the weir to its downstream was between 0.252 and 0.461.

Blocks reduced the maximum scour depth by an average of 55.7% (rectangular), 32.2% (trapezoidal), and 11.3% (circular) compared to weirs without blocks. Block presence increased the maximum scour depth distance from the weir toe by an average of 21.1% (rectangular), 15% (trapezoidal), and 8.3% (circular). The shapes of the blocks did not have much effect on the height of the hill created downstream of the weir. Also, the blocks lowered scouring in the weir toe. Rectangular blocks offered the lowest scour index, indicating the least risk of failure. Scour depth in this study was lower than the values reported for some A-type PKWs. Further, the downstream scour slope of C type PKWs differed from other PKWs and followed a cosine curve. The reason can vary for different boundary conditions. Larger bed material particle size led to a significant decline in the scour depth. For example, with a 53.3% increase in the diameter of the bed material, the maximum scour depth dropped by 28.1%. The reason could be the lower impact of shear stress in gravel beds than in sand beds.

Nomenclature

B: sidewall length
C: the weir with circular blocks
d_{50}: the average particle diameter of the bed material
E_L: energy loss
E_1: the upstream energy
E_2: the downstream energy
Fr: Froude number
Frd: densimetric Froude number
g: gravitational acceleration
H: the upstream flow depth at the weir along with the kinetic energy head
h: the upstream flow depth at the weir
K_1: a constant coefficient for calculating the maximum scour depth
K_2: a constant coefficient for calculating the distance of the maximum scour depth from the weir toe
L: weir crest length
N: the weir without blocks
P: the weir height
P_d: the height of the bed material
Q: the flow rate
q: the discharge per unit width
R: the weir with rectangular blocks
Re: Reynolds number
S: the shape function of the block
S_i: scour index
T: the weir with trapezoidal blocks
T_s: the weir thickness
V_1: upstream flow velocity
V_2: downstream flow velocity
We: Weber number
W_i: inlet key width
W_o: outlet key width
X_s: the distance of maximum scour depth from the weir toe
Y: the tailwater depth at the weir along with the kinetic energy head
y_t: the tailwater depth at the weir
Z_s: the maximum scour depth
ΔH: the difference in flow head upstream and downstream of the weir
μ: dynamic viscosity
ρ_w: water density
ρ_s: bed material density
σ: the surface tension coefficient
σ_g: the uniformity coefficient for bed materials

References

[1] Bodaghi, E., Abdi-Chooplou, C., Ghodsian, M. "Experimental investigation of scour downstream of a type A trapezoidal piano key weir under free and submerged flow conditions", Journal of Hydrology and Hydromechanics, 72(1), pp. 34–48, 2024. https://doi.org/10.2478/johh-2023-0041

[2] Safarzadeh, A., Noroozi, B. "Three-dimensional hydrodynamics of arced piano key spillways", Journal of Hydraulics, 9(3), pp. 61–79, 2014. https://doi.org/10.30482/JHYD.2014.10176

[3] Palermo, M., Crookston, B., Pagliara, S. "Analysis of Equilibrium Morphologies Downstream of a PK Weir Structure", World Environmental and Water Resources Congress 2020, Henderson, NV, USA, 2020, pp. 43–51 ISBN 9780784482940 https://doi.org/10.1061/9780784482971.005

[4] Bhukya, R. K., Pandey, M., Valyrakis, M., Michalis, P. "Discharge Estimation over Piano Key Weirs: A Review of Recent Developments", Water, 14(19), 3029, 2022. https://doi.org/10.3390/w14193029

[5] Jüstrich, S., Pfister, M., Schleiss, A. J. "Mobile Riverbed Scouring Downstream of a Piano Key Weir", Journal of Hydraulic Engineering, 142(11), 04016043, 2016. https://doi.org/10.1061/(ASCE)HY.1943-7900.0001189

[6] Ghafouri, A., Ghodsian., M., Abdi Chooplou, C. "Experimental Study on the Effects of Discharge and Tailwater Depth on Bed Topography Downstream of a Trapezoidal Piano Key Weir", Journal of Hydraulics, 15(3), pp. 107–122, 2020. https://doi.org/10.30482/jhyd.2020.236770.1465

[7] Bodaghi, E., Ghodsian, M., Abdi Chooplou, C. "The Experimental Study of Downstream Scouring of Trapezoidal Piano Key Weir Type A Under Free and Submerged Flow", Journal of Hydraulics, 18(1), pp. 1–18, 2023. https://doi.org/10.30482/jhyd.2022.330389.1590

[8] Dehghan, M., Karami, H. "Numerical investigation of scour downstream of piano key Weirs using Flow-3D software", Amirkabir Journal of Civil Engineering, 56(2), pp. 45–48, 2024. https://doi.org/10.22060/ceej.2024.22659.8019

[9] Gohari, S., Ahmadi, F. "Experimental Study of Downstream Scour of Piano Key Weirs", Journal of Water and Soil Conservation, 26(1), pp. 91–109, 2019. https://doi.org/10.22069/jwsc.2019.14680.2961

[10] Yazdi, A. M., Hoseini, S. A., Nazari, S., Amanian, N. "Comparison of Downstream Scour of the Rectangular and Trapezoidal Piano Key Weirs", Journal of Hydraulics, 15(2), pp. 95–112, 2020. https://doi.org/10.30482/jhyd.2020.227522.1453

[11] Ghodsian, M., Abdi Chooploo, C., Ghafouri, A. "Scouring Downstream of Triangular and Trapezoidal Pianos Key Weirs", Journal of Hydraulics, 16(2), pp. 43–58, 2021. https://doi.org/10.30482/jhyd.2021.261439.1497

[12] Jamal, A. A., Tahaa, K. Y., Hayawi, G. A. A.-M. "Experimental Study of Scour Downstream Piano Key Weir Type C with Changing Height of Weir Width of Keys and Apron Solid", Al-Rafidain Engineering Journal (AREJ), 27(1), pp. 193–204, 2022. https://doi.org/10.33899/rengj.2021.130402.1101

[13] Dehrashid, F. A., Gohari, S., Asim, T., Mishra, R., Khoshkonesh, A., Bahamanpouri, F., Nsom, B. "Experimental and Numerical Study of Local Scouring Downstream of D-Type Piano Key Weir", International Journal of COMADEM, 25(1), pp. 51–62, 2022.

[14] Yazdi, A. M., Hoseini, S., Nazari, S., Fazeli, M. "Numerical and experimental analysis of scour downstream of piano key weirs", Sādhanā, 47(4), 189, 2022. https://doi.org/10.1007/s12046-022-01960-w

[15] Abdi Chooplou, C., Ghodsian, M., Ghafouri, A. "Local scour downstream of various shapes of piano key weirs", Innovative Infrastructure Solutions, 9(4), 117, 2024. https://doi.org/10.1007/s41062-024-01411-x

[16] Kumar, B., Ahmad, Z. "Scour Downstream of a Piano Key Weir With and without a Solid Apron", Journal of Irrigation and Drainage Engineering, 148(1), 04021066, 2022. https://doi.org/10.1061/(ASCE)IR.1943-4774.0001647

[17] Lantz, W., Crookston, B. M., Palermo, M. "Apron and Cutoff Wall Scour Protection for Piano Key Weirs", Water, 13(17), 2332, 2021. https://doi.org/10.3390/w13172332

[18] Rdhaiwi, A. Q., Khoshfetrat, A., Fathi, A. "Experimental investigation of scour downstream of a C-Type trapezoidal piano key weir with stilling basin", Journal of Engineering and Sustainable Development, 27(6), pp. 688–697, 2023. https://doi.org/10.31272/jeasd.27.6.2

[19] Abdi Chooplou, C., Ghodsian, M., Abediakbar, D., Ghafouri, A. "An experimental and numerical study on the flow field and scour downstream of rectangular piano key weirs with crest indentations", Innovative Infrastructure Solutions, 8(5), 140, 2023. https://doi.org/10.1007/s41062-023-01108-7

[20] Fathi, A., Abdi Chooplou, C., Ghodsian, M. "Local scour downstream of type-A trapezoidal stepped piano key weir in sand and gravel sediments", ISH Journal of Hydraulic Engineering, 30(4), pp. 417–429, 2024. https://doi.org/10.1080/09715010.2024.2353612

[21] Kazerooni, S., Abdi Chooplou, C., Ghodsian, M. "Effects of flow splitters on local scour downstream of type-A trapezoidal piano key weir", Applied Water Science, 14(12), 247, 2024. https://doi.org/10.1007/s13201-024-02309-w

[22] Abdi Chooplou, C., Kahrizi, E., Fathi, A., Ghodsian, M., Latifi, M. "Baffle-Enhanced Scour Mitigation in Rectangular and Trapezoidal Piano Key Weirs: An Experimental and Machine Learning Investigation", Water, 16(15), 2133, 2024. https://doi.org/10.3390/w16152133

[23] Sumer, B. M., Fredsoe, J. "Onset of scour below a pipeline exposed to waves", In: 1st International Offshore and Polar Engineering Conference, Edinburgh, UK, 1991, pp. 91–104. ISBN 0-9626104-5-3

[24] Fathi, A., Khoshfetrat, A., Talebipour, F. Z., Saadat, M. "Influence of rigid vegetation on flow energy dissipation downstream of type B trapezoidal piano key weirs", Innovative Infrastructure Solutions, 10(8), 374, 2025. https://doi.org/10.1007/s41062-025-02172-x

[25] Fathi, A., Abdi Chooplou, C., Ghodsian, M. "An Experimental Study of Flow Energy Loss in Trapezoidal Stepped Piano Key Weirs (PKWs)", Modares Civil Engineering Journal, 23(4), pp. 163–174, 2023. https://doi.org/10.22034/23.4.163

[26] Kabiri-Samani, A., Javaheri, A. "Discharge coefficients for free and submerged flow over Piano Key weirs", Journal of Hydraulic Research, 50(1), pp. 114–120, 2012. https://doi.org/10.1080/00221686.2011.647888

[27] Brown, C., Crowley, R. "United States Bureau of Reclamation Type IX Baffled Chute Spillways: A New Examination of Accepted Design Methodology Using CFD and Monte Carlo Simulations, Part I", Proceedings, 7(1), 13, 2019. https://doi.org/10.3390/ECWS-3-05805

[28] Babakhah, L., Khoshfetrat, A. "Investigating local scour downstream of Piano key weir with Riprap", Innovative Infrastructure Solutions, 9(11), 447, 2024. https://doi.org/10.1007/s41062-024-01759-0

[29] Zhou, K., Duan, J. G., Bombardelli, F. A. "Experimental and Theoretical Study of Local Scour around Three-Pier Group", Journal of Hydraulic Engineering, 146(10), 04020069, 2020. https://doi.org/10.1061/(ASCE)HY.1943-7900.0001794

[30] Fathi, A., Khoshfetrat, A., Alavi, S. H. "Downstream Local Scour of PKW with Different Shapes and Numbers of Flow Splitters", Journal of Hydraulic Engineering, 151(4), 04025015, 2025. https://doi.org/10.1061/JHEND8.HYENG-14143

[31] Sajadi, S. M. "Effect of baffled outlet keys at Piano Key Weir on dissipating energy", Irrigation and Drainage Structures Engineering Research, 18(69), pp. 77–92, 2017. https://doi.org/10.22092/aridse.2017.108456.1165

[32] Al-Shukur, A.-H. K., Al-Khafaji, G. H. "Experimental study of the hydraulic performance of piano key weir", International Journal of Energy and Environment, 9(1), pp. 63–70, 2018.

[33] Naghibzadeh, S. M., Heidarnezhad, M., Masjedi, A., Bordbar, A. "Experimental and Numerical Analysis of Energy Dissipation in Piano Key Weirs with Stepped and Baffled Barriers at Downstream Slop", Iranian Journal of Soil and Water Research, 51(10), pp. 2431–2442, 2021. https://doi.org/10.22059/ijswr.2020.295541.668467

[34] Eslinger, K. R., Crookston, B. M. "Energy Dissipation of Type a Piano Key Weir", Water, 12(5), 1253, 2020. https://doi.org/10.3390/w12051253

[35] Singh, D., Kumar, M. "Gene expression programming for computing energy dissipation over type-B piano key weir", Renewable Energy Focus, 41, pp. 230–235, 2022. https://doi.org/10.1016/j.ref.2022.03.005

[36] Shen, X., Oertel, M. "Influence of Piano Key Weir Crest Shapes on Flow Characteristics, Scale Effects, and Energy Dissipation for In-Channel Application", Journal of Hydraulic Engineering, 149(6), 04023010, 2023. https://doi.org/10.1061/JHEND8.HYENG-13322

[37] Rdhaiwi, A. Q., Khoshfetrat, A., Fathi, A. "Experimental comparison of flow energy loss in type-B and -C trapezoidal piano key weirs (PKWs)", Journal of Engineering and Sustainable Development, 28(1), pp. 55–64, 2024. https://doi.org/10.31272/jeasd.28.1.4

[38] Hoffmans, G. J. C. M. "Jet Scour in Equilibrium Phase", Journal of Hydraulic Engineering, 124(4), pp. 430–437, 1998. https://doi.org/10.1061/(ASCE)0733-9429(1998)124:4(430)

[39] Farooq, R., Ghumman, A. R., Tariq, M. A. U. R., Ahmed, A., Jadoon, K. Z. "Optimal Octagonal Hooked Collar Countermeasure to Reduce Scour Around a Single Bridge Pier", Periodica Polytechnica Civil Engineering, 64(4), pp. 1026–1037, 2020. https://doi.org/10.3311/PPci.15966

[40] Khajavi, M., Kashefipour, S. M., Shafai Bejestan, M. "Bridge Abutment Protection against Scouring for Unsteady Flow Conditions", Periodica Polytechnica Civil Engineering, 66(1), pp. 310–322, 2022. https://doi.org/10.3311/PPci.18892

[41] Bormann, N. E., Julien, P. Y. "Scour Downstream of Grade-Control Structures", Journal of Hydraulic Engineering, 117(5), pp. 579–594, 1991. https://doi.org/10.1061/(ASCE)0733-9429(1991)117:5(579)

[42] Gumgum, F., Guney, M. S. "Time Dependent Live-bed Scour Around Circular Piers under Flood Waves", Periodica Polytechnica Civil Engineering, 64(1), pp. 65–72, 2020. https://doi.org/10.3311/PPci.14664

[43] Hassanzadeh, Y., Jafari-Bavil-Olyaei, A., Taghi-Aalami, M., Kardan, N. "Meta-heuristic Optimization Algorithms for Predicting the Scouring Depth Around Bridge Piers", Periodica Polytechnica Civil Engineering, 63(3), pp. 856–871, 2019. https://doi.org/10.3311/PPci.12777

[44] Palermo, M., Pagliara, S., Bombardelli, F. A. "Theoretical Approach for Shear-Stress Estimation at 2D Equilibrium Scour Holes in Granular Material due to Subvertical Plunging Jets", Journal of Hydraulic Engineering, 146(4), 04020009, 2020. https://doi.org/10.1061/(ASCE)HY.1943-7900.0001703

[45] Verma, D. V. S., Goel, A. "Stilling Basins for Pipe Outlets Using Wedge-Shaped Splitter Block", Journal of Irrigation and Drainage Engineering, 126(3), pp. 179–184, 2000. https://doi.org/10.1061/(ASCE)0733-9437(2000)126:3(179)

[46] Mshali, K. C., Khoshfetrat, A., Fathi, A. "Experimental study of the effect of jump on the Downstream Scouring of type-C trapezoidal piano key weir", Amirkabir Journal of Civil Engineering, 56(11), pp. 1353–1368, 2025. https://doi.org/10.22060/ceej.2024.22565.7996

[47] Lantz, W. D., Crookston, B. M., Palermo, M. "Evolution of local scour downstream of Type A PK weir in non-cohesive sediments", Journal of Hydrology and Hydromechanics, 70(1), pp. 103–113, 2022. https://doi.org/10.2478/johh-2021-0035